Chapter 6

Appendix 6C: Christiaan Huygens and Phase-Locked Pendulum Clocks

Notions of the phase-lock concept first originated with the pendulum clocks of Christiaan Huygens as described earlier in Section 1.1.1. This section takes a brief detour into the world of pendulum clocks and the entrainment of one oscillator to a master; i.e., phase-locking. Characterization of the single pendulum case is considered first.

6C.1 Single Pendulum

An ideal classical pendulum is shown in Figure 6C-1. Assuming that the pendulum arm is rigid and has no mass, it is convenient to think about the motion of the pendulum bob in terms of motion along the fixed radius R where the angle φ is a function of time. The tangential force perpendicular to *R* that is created by the weight of the pendulum bob is given by

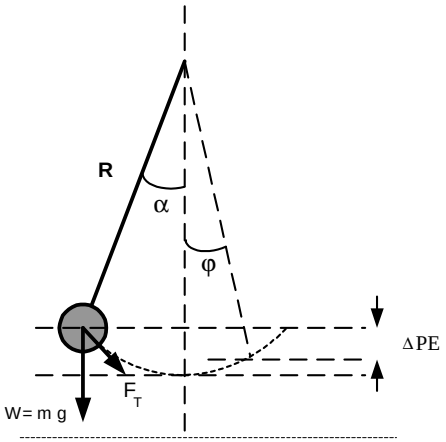

Figure 6C-1 Classical pendulum.

m mass of pendulum
R length of pendulum
G acceleration of gravity (e.g., 9.81 m/s^2)
α starting angle

$$F_T = mg\sin(\varphi) \tag{6C.1}$$

From Newton's laws of motion, this tangential force must be associated with the tangential acceleration

$$\begin{aligned} F_T &= ma_T = m\left(\frac{dv_T}{dt}\right) \\ &= m\frac{d}{dt}\left(R\frac{d\varphi}{dt}\right) \\ &= mR\frac{d^2\varphi}{dt^2} \end{aligned} \tag{6C.2}$$

Proper attention to signs for the forces involved results in the describing differential equation in terms of φ given by

$$\frac{d^2\varphi}{dt^2} + \frac{g}{R}\sin(\varphi) = 0 \tag{6C.3}$$

Any real-world pendulum will experience damping due to air resistance and other mechanical inefficiencies. This can be included in the model by adding an additional term to (6C.3) that is proportional to $d\varphi/dt$, and in the case where the oscillation is forced (for phase-locking purposes), this homogeneous equation can be further augmented with a driving source as

$$\frac{d^2\varphi}{dt^2} + D\frac{d\varphi}{dt} + \frac{g}{R}\sin(\varphi) = A\sin(\omega_d t + \phi) \tag{6C.4}$$

Returning to the homogenous lossless case (6C.3), if the angular extents for the pendulum swing are kept small, the usual small-angle approximation $\sin(\varphi) \approx \varphi$ can be made which leads to the simple differential equation

$$\frac{d^2\varphi}{dt^2} + \frac{g}{R}\varphi = 0 \tag{6C.5}$$

The solution to this differential equation is clearly a sinusoid, and after substitution of $\varphi(t) = B\sin(\omega_o t)$ into (6C.5), the validity of this solution is immediately seen where the correct solution demands that the natural radian frequency of the oscillation be given by

$$\omega_o = \sqrt{\frac{g}{R}} \tag{6C.6}$$

Returning now to the original nonlinear differential equation (6C.3), an exact solution can be found by first multiplying both sides of the equation by $d\varphi/dt$ which creates

$$\left(\frac{d^2\varphi}{dt^2}\right)\frac{d\varphi}{dt} = -\omega_o^2\sin(\varphi)\frac{d\varphi}{dt} \tag{6C.7}$$

Integrating both sides of (6C.7) with respect to time results in

$$\frac{1}{2}\left(\frac{d\varphi}{dt}\right)^2 - \omega_o^2\cos(\varphi) = k_o \tag{6C.8}$$

where k_o is a constant of integration. Assuming that the pendulum has a maximal displacement angle $\varphi_{max} = \alpha$, then $\varphi'(\alpha) = 0$. Solving for the time-derivative and taking the positive root leads to

$$\frac{d\varphi}{dt} = \omega_o\sqrt{2\left[\cos(\varphi) - \cos(\alpha)\right]} \tag{6C.9}$$

Integrating one more time produces

$$\int \frac{d\varphi}{\sqrt{2\left[\cos(\varphi) - \cos(\alpha)\right]}} = \omega_o t \tag{6C.10}$$

The time required for φ to increase from 0 to α corresponds to ¼ of a complete pendulum cycle and is given by

$$\frac{T_{pen}}{4} = \sqrt{\frac{R}{2g}} \int_0^{\alpha} \frac{d\varphi}{\sqrt{\cos(\varphi) - \cos(\alpha)}} \tag{6C.11}$$

Using the identities $\cos(\varphi) = 1 - 2\sin^2(\varphi/2)$ and $\cos(\alpha) = 1 - 2\sin^2(\alpha/2)$ in (6C.11), the oscillation period for the pendulum T_{pen} can be rewritten as

$$T_{pen} = 2\sqrt{\frac{R}{g}} \int_0^{\alpha} \frac{d\varphi}{\sqrt{k^2 - \sin^2(\varphi/2)}} \tag{6C.12}$$

with $k = \sin(\alpha/2)$. A new variable of integration can be defined as $k\sin(\theta) = \sin(\varphi/2)$ with the differentials being inter-related as

$$\cos\left(\frac{\varphi}{2}\right)\frac{d\varphi}{2} = k\cos(\theta)\,d\theta \tag{6C.13}$$

After some additional algebraic re-arrangement, the differential becomes

$$d\varphi = \frac{2k\cos(\theta)\,d\theta}{\cos\left(\frac{\varphi}{2}\right)} = \frac{2\sqrt{k^2 - \sin^2(\varphi/2)}}{\sqrt{1 - k^2\sin^2(\theta)}} \tag{6C.14}$$

Substitution of (6C.14) into (6C.12) leads to the final result for the pendulum swing time period as

$$T_{pen} = 4\sqrt{\frac{R}{g}} \int_0^{\pi/2} \frac{d\theta}{\sqrt{1 - k^2\sin^2(\theta)}} \tag{6C.15}$$

Aside: Conservation of energy may be used to quickly arrive at the same starting point represented by (6C.3). The change of potential energy that occurs from angular position α to φ can be equated to the increase in kinetic energy (since the bob is momentarily motionless at angular position α) as

$$\frac{1}{2}mv^2 = mgR\left[\cos(\varphi) - \cos(\alpha)\right] \tag{6C.16}$$

Since the velocity v must be tangential to the arc that is scribed by the bob, at any instant in time $v = R(d\varphi/dt)$. Substituting this into (6C.16) leads directly to (6C.3).

The integral involved in (6C.15) is an elliptic integral of the first kind. With $k = \sin(\alpha/2)$, the integral is very well behaved because k is always $< (\sqrt{2})/2$. In the case of elliptic filters, however, k is often very close to unity thereby making numerical evaluation of (6C.15) considerably more challenging.

The elliptic integral of the first kind is generally presented as

$$F\left(k,x\right)=\int_{0}^{x}\frac{d\theta}{\sqrt{1-k^{2}\sin^{2}\left(\theta\right)}} \tag{6C.17}$$

with the complete elliptic integral of the first kind given by $F(k, \pi/2)$. It is possible to show that

$$T_{pen}=2\pi\sqrt{\frac{R}{g}}\left[1+\left(\frac{1}{2}\right)^{2}k^{2}+\left(\frac{1\times3}{2\times4}\right)^{2}k^{4}+\left(\frac{1\times3\times5}{2\times4\times6}\right)^{2}k^{6}+\ldots\right] \tag{6C.18}$$

Visual inspection of (6C.18) reveals that the series is slow to converge when k is reasonably close to unity, and this motivates finding an improved method to calculate $F(k, x)$.

Convergence speed and accuracy can be dramatically enhanced by making use of a recursive relationship known as *Gauss's transformation*.[1] This relationship can be used to expand the elliptic integral (6C.17) into a recursive series where

$$F\left(\varphi,k\right)=\left(1+k_{1}\right)F\left(\phi_{1},k_{1}\right) \tag{6C.19}$$

This expansion can be repeatedly applied ultimately leading to

$$\lim_{p\to\infty}F\left(\phi_{p},k_{p}\right)=\frac{\pi}{2} \tag{6C.20}$$

The expansion generally converges to 10 or more decimal place accuracy within only a few iterations of (6C.19). The other formulas that accompany (6C.19) are given by

$$\begin{aligned} k' &= \sqrt{1-k^{2}} \\ k_{1} &= \frac{1-k'}{1+k'} \\ \phi_{1} &= \arcsin\left[\frac{\left(1+k'\right)\sin\left(\phi\right)}{1+\sqrt{1-k^{2}\sin^{2}\left(\phi\right)}}\right] \end{aligned} \tag{6C.21}$$

In the case where the complete elliptic integral of the first kind is to be computed (i.e., $\varphi = \pi/2$), a different set of recursive formulas [1] can be used to compute the result with even less effort than with (6C.21). This result is given by

$$\begin{aligned} a_{i+1} &= \frac{a_{i}+b_{i}}{2} \\ b_{i+1} &= \sqrt{a_{i}b_{i}} \end{aligned} \tag{6C.22}$$

with

$$\begin{aligned} a_{0} &= 1+k \\ b_{0} &= 1-k \end{aligned} \tag{6C.23}$$

[1] Also referred to as *Landen's transformation.*

and after sufficient convergence, computing

$$F\left(\frac{\pi}{2},k\right)=\frac{\pi}{2a_n} \tag{6C.24}$$

These results can be used to compare the pendulum's true period of oscillation (given by equation (6C.15)) with the linear result represented by (6C.6) as shown in Figure 6C-2. The linear theory and exact theory agree very closely for small angular swings as shown in the figure.

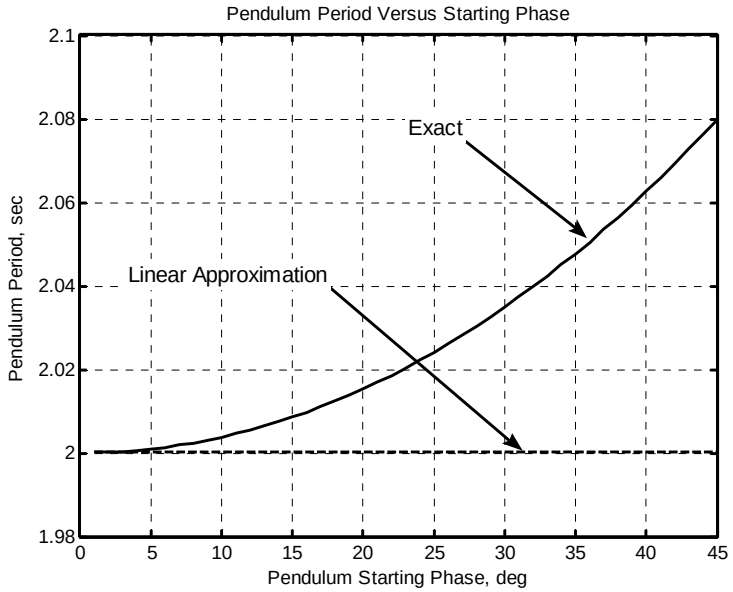

Figure 6C-2 Single pendulum swing period versus starting phase angle[2] (R = 0.993961m).

6C.1.1 Time Domain Solution of the Single Pendulum Problem

The mathematics are simplified if the linearized model represented by (6C.5) is used rather than the complete nonlinear model. For the linearized case, the time-period for the pendulum's motion is given by (6C.6) with the pendulum's motion being precisely sinusoidal. A very accurate approximate solution for the complete nonlinear problem is given by assuming this same sinusoidal motion, but using the time-period given by (6C.15). In all but the most rigorous situations, this solution is adequately precise.

Numerical integration is normally the solution method used to solve the more general nonlinear differential equation given by (6C.3). Although the integration methods within programming packages like MATLAB can be used to solve (6C.3), engineers often resort to a brute-force application of Newton's method (i.e., forward Euler method) which is fairly inaccurate compared to the many alternatives available for solving this problem. Numerical integration accuracy is an important topic that is developed at length in [2] so only a few methods are considered here: (i) the forward Euler method which is often used but not recommended, (ii) the backward Euler method, (iii) the second-order Runge-Kutta method, and (iv) the fourth-order Runge-Kutta method.

[2] Book CD: \CD_Ch6\Pendulums\u12627_pendulums_main.m.

Forward Euler Integration

Although prone to accuracy and stability issues, the forward Euler (FE) method is often used for solving differential equations because it is simple to use. The forward Euler method is an explicit integration method as discussed in [3] and [4]. In this method, the time-derivative is approximated as

$$s'(t) \approx \frac{s(t+h)-s(t)}{h} \tag{6C.25}$$

where the simulation time increment is given by *h*. Focusing on the original differential equation (6C.3), it is simple to recast this second-order differential equation as a pair of first-order differential equations by defining

$$\begin{aligned} U1(t) &= \varphi(t) \\ U2(t) &= \frac{d\varphi}{dt} \end{aligned} \tag{6C.26}$$

leading to

$$\begin{aligned} \frac{dU2}{dt} &= -\frac{g}{R}\sin(U1) \\ \frac{dU1}{dt} &= U2 \end{aligned} \tag{6C.27}$$

Substituting (6C.25) into (6C.27) results in

$$\begin{aligned} \frac{U2_{n+1}-U2_n}{h} &= -\frac{g}{R}\sin(U1_n) \\ \frac{U1_{n+1}-U1_n}{h} &= U2_n \end{aligned} \tag{6C.28}$$

where the index *n* represents the value of the given parameter at time $t = nh$ and *h* is the constant time step used. Solving (6C.28) for the parameter values at the next time step $n + 1$ produces

$$\begin{aligned} U2_{n+1} &= U2_n + \left(-\frac{gh}{R}\right)\sin(U1_n) \\ U1_{n+1} &= U1_n + U2_n h \end{aligned} \tag{6C.29}$$

The fact that the FE method is an explicit method results in only time-index *n* values being on the right side of the equal signs and the $n + 1$ (future) time index values being on the left-hand side.

This set of difference equations can be easily programmed and sample results are shown in Figure 6C-3. Due to numerical imprecision even with $h = 30$ msec, the computed solution slowly grows in amplitude rather than remaining constant-envelope as it should. Error propagation with the forward Euler method is so poor that the amplitude growth is difficult to avoid even with a much smaller choice for *h*. As mentioned earlier, the FE method is *not recommended* due to its poor accuracy and stability limitations.

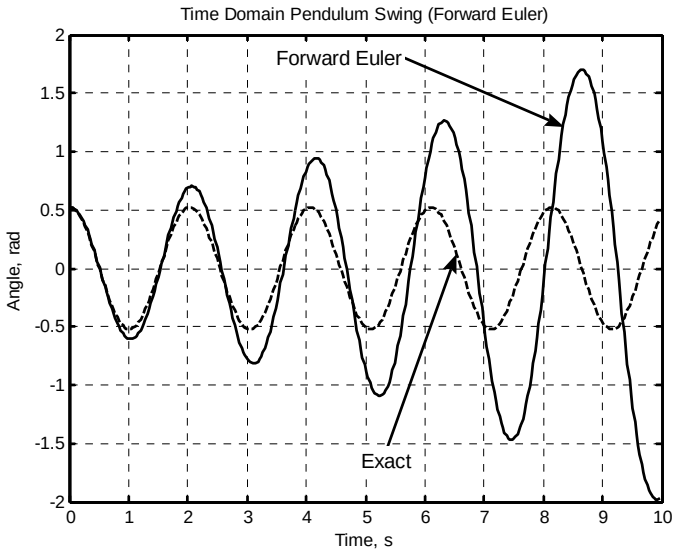

Figure 6C-3 Forward Euler differential equation solution[3] (h = 0.03s, φ_0 = 30°, R = 0.993961m).

Backward Euler Method

The backward Euler (BE) method is an implicit integration method and as such, it is not possible to use this method without solving a nonlinear equation at each step unless the differential equation is linearized as in (6C.5). Although this linearization step is undesirable for comparison purposes with the other methods considered here, it is still sufficient to illustrate the greater stability properties of this method as compared to the FE method.

The BE method results in the state equations given by

$$\begin{aligned} U2_{n+1} &= U2_n - \frac{gh}{R}U1_{n+1} \\ U1_{n+1} &= U1_n + hU2_{n+1} \end{aligned} \tag{6C.30}$$

and these can be recast in matrix form as

$$\begin{bmatrix} \frac{gh}{R} & 1 \\ 1 & -h \end{bmatrix} \begin{bmatrix} U1_{n+1} \\ U2_{n+1} \end{bmatrix} = \begin{bmatrix} U2_n \\ U1_n \end{bmatrix} \tag{6C.31}$$

Solving this for the next-step state-variable values,

$$\begin{bmatrix} U1_{n+1} \\ U2_{n+1} \end{bmatrix} = \frac{\begin{bmatrix} h & 1 \\ 1 & -\frac{gh}{R} \end{bmatrix} \begin{bmatrix} U2_n \\ U1_n \end{bmatrix}}{1+\frac{gh^2}{R}} \tag{6C.32}$$

[3] Book CD: \Ch6\Pendulums\u12627_pendulums_main.m.

This set of simultaneous difference equations can be programmed leading to the results shown in Figure 6C-4. In the BE method case, the numerical imprecision leads to a decay in the envelope magnitude as shown in Figure 6C-4, so although this is a more stable solution, the extent of the numerical error is about the same as for the FE method.

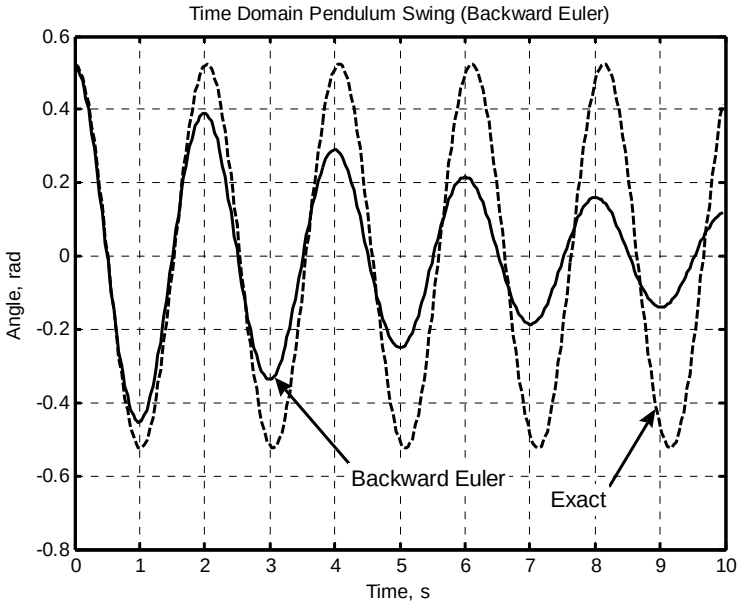

Figure 6C-4 Backward Euler differential equation solution[4] (h = 0.03s, φ_0 = 30°, R = 0.993961m).

Second-Order Runge-Kutta Method

The derivation of the Runge-Kutta method is beyond the scope of this text, but interested readers may refer to [3] and [5]. The formula for the second-order Runge-Kutta (RK2) solution to a second-order differential equation is given by

$$\begin{aligned} k_1 &= f\left(t_n, x_n, y_n\right) \\ j_1 &= g\left(t_n, x_n, y_n\right) \\ k_2 &= f\left(t_n + \frac{h}{2}, x_n + \frac{h}{2}k_1, y_n + \frac{h}{2}j_1\right) \\ j_2 &= g\left(t_n + \frac{h}{2}, x_n + \frac{h}{2}k_1, y_n + \frac{h}{2}j_1\right) \\ x_{n+1} &= x_n + hk_2 \\ y_{n+1} &= y_n + hj_2 \end{aligned} \tag{6C.33}$$

In the context of the present differential equation of interest (6C.3), the RK2 solution is given by

[4] Book CD: \Ch6\Pendulums\u12627_pendulums_main.m.

$$\begin{aligned} U1(t) &= \varphi(t) \\ U2(t) &= \frac{d\varphi}{dt} \\ \frac{dU2}{dt} &= f(\ldots) = -\frac{g}{R}\sin(U1) \\ \frac{dU1}{dt} &= g(\ldots) = U2 \end{aligned} \tag{6C.34}$$

With some additional simplification, the final recursive solution can be written as

$$\begin{aligned} k_1 &= -\frac{g}{R}\sin(U1_n) \\ j_1 &= U2_n \\ k_2 &= -\frac{g}{R}\sin\left(U1_n + \frac{h}{2}j_1\right) \\ j_2 &= U2_n + \frac{h}{2}k_1 \\ U1_{n+1} &= U1_n + hj_2 \\ U2_{n+1} &= U2_n + hk_2 \end{aligned} \tag{6C.35}$$

These finite difference equations are easily programmed and representative results are shown in Figure 6C-5. As shown in this figure, the results follow the exact solution closely and reasonably good precision is still being delivered at 200 seconds into the simulation. Numerical precision accuracy must always be considered whenever complete closed-form solutions are not available, even with more accurate methods as the RK2 method.

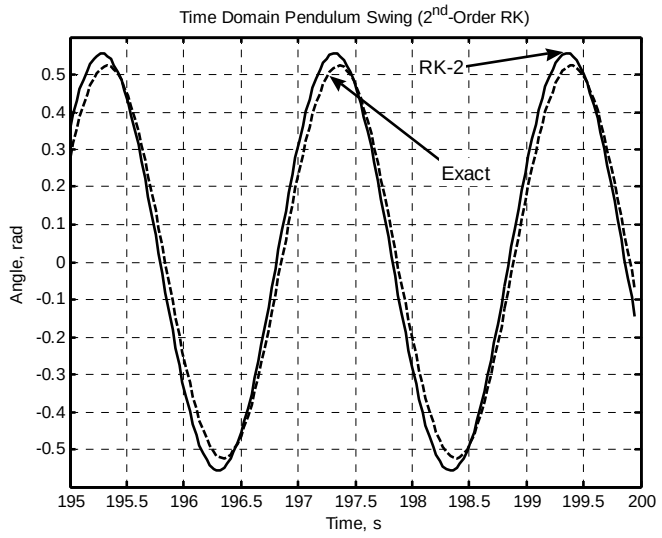

Figure 6C-5 RK2 differential equation solution[5] (h = 0.03s, φ_0 = 30°, R = 0.993961m). Even at t = 200s, the computed and exact solutions are still very similar.

[5] Book CD: \Ch6\Pendulums\u12627_pendulums_main.m.

Fourth-Order Runge-Kutta

In the case of the fourth-order Runge-Kutta (RK4) method, the applicable formulas for solving a first-degree differential equation are given by (6C.36). These equations must be expanded in order to deal with the second-order differential equation that describes the pendulum's motion. Choosing the same assignments for $U1$ and $U2$ as in (6C.34), the set of iterated equations for the RK4 solution are as given by (6C.37).

$$\begin{aligned}
k_1 &= f\left(t_n, x_n\right) \\
k_2 &= f\left(t_n + \frac{h}{2}, x_n + \frac{h}{2}k_1\right) \\
k_3 &= f\left(t_n + \frac{h}{2}, x_n + \frac{h}{2}k_2\right) \\
k_4 &= f\left(t_n + h, x_n + hk_3\right) \\
x_{n+1} &= x_n + \frac{h}{6}\left(k_1 + 2k_2 + 2k_3 + k_4\right)
\end{aligned} \qquad \text{(6C.36)}$$

$$\begin{aligned}
k_1 &= -\frac{g}{R}\sin\left[U1_{n-1}\right] \\
j_1 &= U2_{n-1} \\
k_2 &= -\frac{g}{R}\sin\left[U1_{n-1} + \frac{h}{2}j_1\right] \\
j_2 &= U2_{n-1} + \frac{h}{2}k_1 \\
k_3 &= -\frac{g}{R}\sin\left[U1_{n-1} + \frac{h}{2}j_2\right] \\
j_3 &= U2_{n-1} + \frac{h}{2}k_2 \\
k_4 &= -\frac{g}{R}\sin\left[U1_{n-1} + hj_3\right] \\
j_4 &= U2_{n-1} + hk_3 \\
U1_n &= U1_{n-1} + \frac{h}{6}\left(j_1 + 2j_2 + 2j_3 + j_4\right) \\
U2_n &= U2_{n-1} + \frac{h}{6}\left(k_1 + 2k_2 + 2k_3 + k_4\right)
\end{aligned} \qquad \text{(6C.37)}$$

This set of difference equations leads to the results shown in Figure 6C-6. As shown in this figure, the computed results match the ideal results almost exactly even at 1,500 seconds into the time simulation.

Although other techniques may be superior to the Runge-Kutta methods explored here, the simplicity of the method combined with the very good precision make it a highly recommended method for use in solving differential equations numerically.

6C.1.2 Phase-Locked Oscillator

External force can be impressed on the pendulum's motion in a number of ways in order to illustrate the phase-entrapment (phase-locking) process. The method that is used here is based on revisiting the foundational differential equation (6C.4). Rather than leave the bob's motion up to self-autonomous action due to gravity alone, an additional tangential force that acts on the bob is impressed by $A\sin(\omega_d t + \phi)$ in (6C.4). In this form, the linearized system has a characteristic equation given by

$$s^2 + \frac{D}{R}s + \frac{g}{R} = 0 \qquad \text{(6C.38)}$$

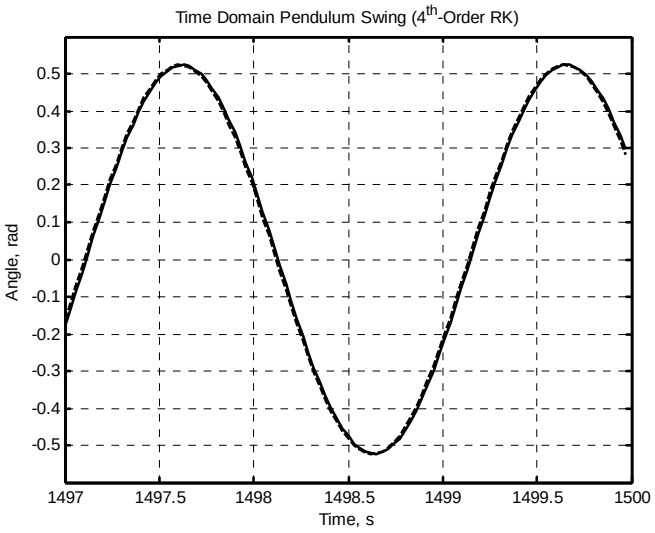

Figure 6C-6 RK4 differential equation solution[6] (h = 0.03s, φ_0 = 30°, R = 0.993961m). Even at t = 1,500s, the computed and exact solutions are still virtually identical.

with the natural frequency given again by (6C.6) and a damping factor given by

$$\zeta = \frac{D}{2}\sqrt{\frac{1}{gR}} \tag{6C.39}$$

The damping factor ζ combined with the magnitude and frequency of the external force strongly dictate how the oscillator becomes entrapped by the external force over time as shown in Figure 6C-7 and Figure 6C-8. These figures illustrate how the phase error between the pendulum and the applied external force tends to zero over time.

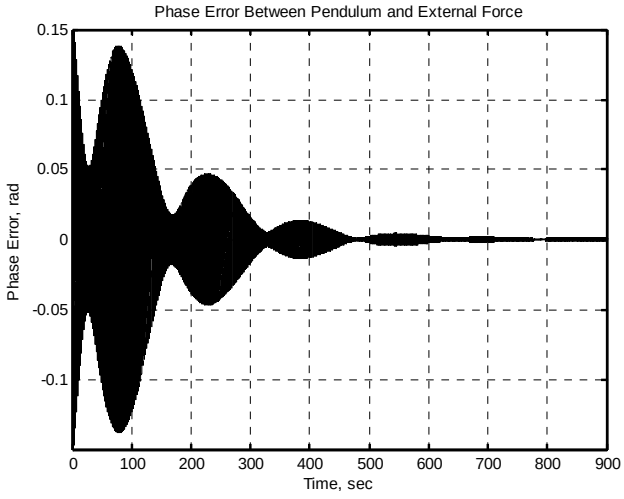

Figure 6C-7 Phase entrapment of oscillator by external master[7] [$\omega_d = 1.005\omega_o$, $A = 0.05\alpha$, $\zeta = 0.0025$ in (6C.4)].

[6] Ibid.
[7] Book CD: \Ch6\Pendulums\u12627_pendulums_main.m.

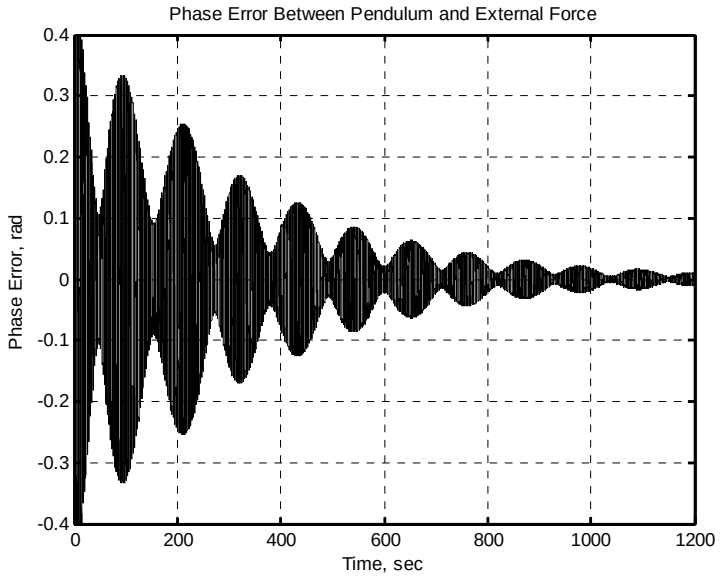

Figure 6C-8 Phase entrapment of oscillator by external master[8] [$\omega_d = 1.005\omega_o$, $A = 0.05\alpha$, $\zeta = 0.001$ in (6C.4)].

In PLL applications, the damping factor takes on a different role, but the PLL and entrapped oscillator are very similar concepts. Both of the previous figures illustrate under-damped transient responses of a second-order system. A clearer picture of the entrapment process can be seen if the phase error is sampled only once per pendulum cycle as shown in Figure 6C-9.

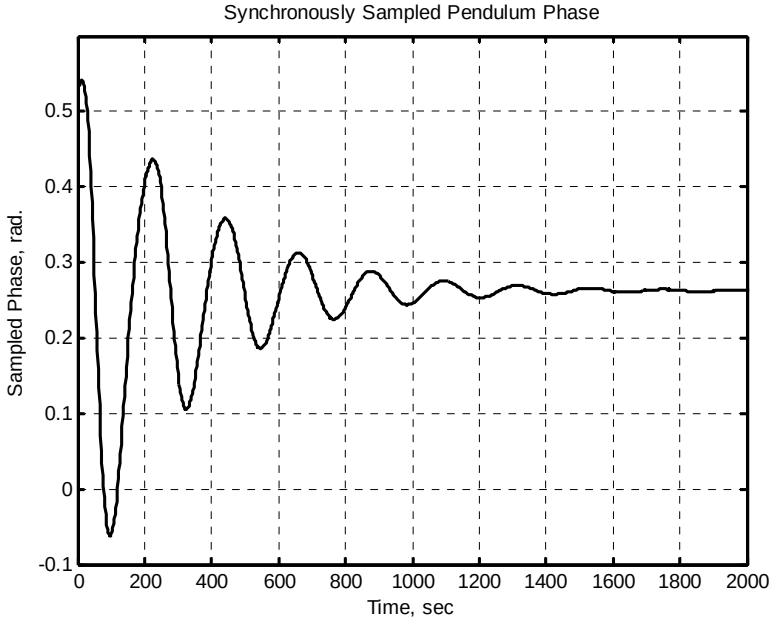

Figure 6C-9 Pendulum phase sampled once per period of the external forcing function.[9] Under-damped second-order transient behavior is clearly visible.

[8] Ibid.
[9] Book CD: \Ch6\Pendulums\u12627_pendulums_main.m.

Key Points:

- The elliptic integral of the first kind can be calculated very efficiently using the Gauss transformation (Landen's formula).
- Although easy to use, the explicit FE method is not recommended due to its poor accuracy and stability characteristics.
- The RK2 and RK4 numerical methods are recommended for solving differential equations numerically.
- Oscillator phase entrapment (i.e., phase-lock) depends strongly on (i) the frequency difference between the free-running oscillator and applied external stimulus, (ii) the magnitude of the external stimulus, and (iii) the damping factor of the oscillator's resonance.

References

[1] Ruckdeschel, F.R., *BASIC Scientific Subroutines*, Vol. 2, Peterborough, NH: BYTE Publications, 1981.

[2] Crawford, J.A., "Advanced Phase-Lock Techniques Applied," working papers, unpublished.

[3] Kreyszig, E., *Advanced Engineering Mathematics*, 3rd ed., New York: John Wiley & Sons, 1972.

[4] Crawford, J.A., *Frequency Synthesizer Design Handbook*, Norwood, MA: Artech House, 1994.

[5] Gerald, C.F., Wheatley, P.O., *Applied Numerical Analysis*, Reading, MA: Addison-Wesley, 1970.